Tricriticality and persistency of trails and silhouettes

1988 J. Phys. A: Math. Gen. 21 3783

(http://iopscience.iop.org/0305-4470/21/19/016)

J. Phys. A: Math. Gen. 21 (1988) 3783-3800. Printed in the UK

Tricriticality and persistency of trails and silhouettes

H A Lim

Supercomputer Computations Research Institute, Florida State University, Tallahassee, FL 32306-4052, USA

Received 7 March 1988, in final form 16 May 1988

Abstract. Trails and silhouettes (polymers with loops) are generated using exact enumeration on a face-centred cubic lattice. By assigning a tunable fugacity factor with each intersection it is observed that, as the fugacity for intersections is increased the trail and silhouette configurations change from swollen to compact ones, indicating the existence of tricritical points. Strong divergence of the specific heats for different path lengths is used to locate these tricritical points. The Dlog Padé scheme is used to compute the corresponding tricritical exponents in the limit of large path lengths. The tricritical exponents thus obtained show that these tricritical points are distinct from the usual Θ point, and that trails and silhouettes do not belong to the SAW universality class. The tricritical exponents further show that trails and silhouettes do not belong to the same universality class.

Persistency arising from fixing the initial step is also investigated and it is found that odd moments of the persistency obey a power law that can be expressed in terms of the critical exponent, ν, and the path length, l.

1. Introduction

Lattice trails are a polymer chain model introduced by Malakis [1]. (For an excellent analytical work on trails on a Bethe lattice see [2].) The model interpolates in a non-trivial way between two problems in statistical mechanics: self-avoiding walks (SAW) and random walks (RW). Just like SAW double occupancy of bonds is forbidden, but in contrast to SAW (and like RW) self-intersections are allowed in trails. The former property leads to the excluded-volume effect and trail configurations tend to remain in a swollen phase. However, if an interaction energy $\epsilon = -|\epsilon|$ (or a fugacity factor $f = \exp(-\epsilon/k_B T) = \exp\theta$) is introduced with each attractive self-intersection, the relative number of intersections may be controlled.

In the limit of $\theta \to -\infty$, intersections are suppressed and the usual SAW configurations are recovered whereas in the limit of $\theta \to \infty$, configurations with the maximal number of intersections will dominate. Intermediate between these limits is a regime of interest: $\theta = 0$ (corresponding to no interaction energy or $T = \infty$). It was first found by Malakis [1] that trails at $T = \infty$ belong to the SAW universality class. Subsequent extensive enumerations on triangular and other lattices were performed and analysed by Guttmann [3]. These results further support the claim that trails at $T = \infty$ belong to the SAW universality class [4].

However, as the temperature is lowered (or θ is increased), the interplay between the excluded-volume and the self-intersecting effects may lead to a collapse transition from a swollen to a compact phase. Such a collapse transition is very reminiscent of the Flory Θ point of linear polymers in poor solvent [5] and of the Θ point of self-attracting SAW [6-16]. All such transitions are expected to be described by tricritical points in the terminology of critical phenomena [6, 16, 17]. But hitherto, only this tricritical Θ point has attracted a lot of attention. In 3D this Θ point is Gaussian up to logarithmic corrections [8, 18-21]. The tricritical point associated with trails, however, has no renormalisation group fixed point associated with it in $\epsilon = 4 - d$ dimensions. Instead, the renormalisation group approach shows that the only stable fixed point is that of SAW [22]. This is unphysical because a tricritical point is always expected between a swollen and a collapse phase [22, 23]. Indeed, as has been shown by earlier enumerations [22, 24], the tricritical behaviour of trails in 3D are non-Gaussian ($\nu_t \neq \frac{1}{2}$, $\gamma_t \neq 1$) at the tricritical point. This constitutes a motivation for studying the tricriticality of such a model which, as emphasised above, is inaccessible by renormalisation group analysis, using a numerical approach. The existing data at this tricritical point are from exact enumeration on a loose-packed simple cubic lattice [22]. These results suffer from the superimposed oscillations due to the interference of the 'antiferromagnetic singularity'. It is therefore of interest to pursue this study further by exact enumeration of trails on a face-centred cubic lattice which is close-packed and does not have these odd-even oscillations.

In a problem related to the trail problem, only silhouettes or shadows of trails are considered. This model is interesting for it possesses tricritical exponents which are different from their trail counterparts [25]. It is also believed that such a model may mimic behaviours of polymers with loops [25-27]. It is important to note that sihouettes, unlike trails, have a renormalisation group fixed point of order $\sqrt{\epsilon}$ in $\epsilon = 4 - d$ dimensions [23]. It is also instructive to compare the tricritical point of silhouettes with that of the usual Flory Θ point or the Θ point of SAW with non-bonded nearest-neighbour interactions [5-16]. The upper critical dimension of the Θ point is $d_u = 3$ and the configurations are Gaussian up to logarithmic corrections [6, 8, 12, 14, 18-21, 28]. The tricritical point of silhouettes, on the other hand, has an upper critical dimension $d_u = 4$ and the 3D configurations are predicted to be non-Gaussian in a $\sqrt{\epsilon}$ expansion up to second order (ϵ) [23, 29]. Perhaps the most striking fact about these results is the unusual deviations from the mean-field exponents to $\gamma_t < 1$ and $\nu_t < \frac{1}{2}$ at the tricritical point in 3D [29].

The study of the tricritical behaviours of the trail and silhouette models will constitute the main subject of this paper. By enumerating the trails and their silhouettes on a close-packed face-centred cubic lattice, we hope to provide possible further support for earlier claims that trails and silhouettes belong to universality classes different from that of the SAW universality class [22, 25]. But due to the exponential growth in the possible number of configurations we are only able to enumerate up to a chain length of 10. This paper is organised as follows: in the next section we take a cursory look at the model and differentiate a trail from its silhouette. We also define all the notations used and the various physical quantities we will study in the same section. Subsection 3.1 presents the results from the enumerations on trails and the results of the analysis are given in § 3.2. Subsection 3.3 deals with persistency arising from fixing the first step. Comparisons with results from self-attracting SAW are also given in § 3.2. The corresponding subsections for silhouettes are given in § 4 and comparisons of trail and silhouette tricritical exponents are also briefly discussed. The last section, § 5, is devoted to conclusions and discussions.

2. Definitions and symbols

2.1. Trails [1]

Trails consist of all configurations of walkers on a lattice which are free to intersect their own path through an already visited site, but are not allowed to go more than once along the same bond. They are directional, as shown in figure 1(*a*). In the terminology of critical phenomena [6], site intersection is an irrelevant perturbation and the trail model belongs to the SAW universality class described by the O(n) spin model in the limit $n \to 0$ [30]. Lucid field-theoretical expositions may be found in [23] and references therein and we shall not reproduce the proofs of the various correspondences here.

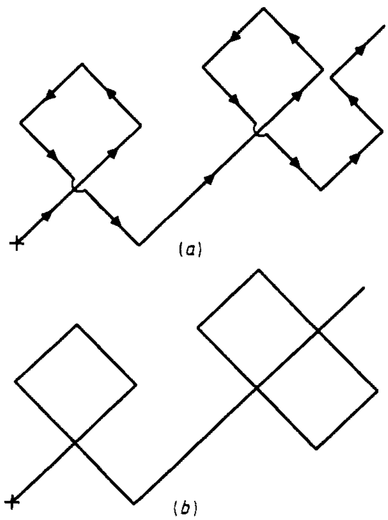

Figure 1. (*a*) A trail with intersections. Associated with each intersection is a factor of e^{θ}; (*b*) the corresponding silhouette.

2.2. Silhouettes [23, 31]

Silhouettes, on the other hand, are the shadows of the trails and are not directional. In other words, silhouettes are an equivalence class obtained from trails when the chronological order of the building bonds are ignored. Thus the mapping from trails to silhouettes is a homomorphism or many-to-one as shown in figures 1 and 2 (i.e. each silhouette is counted once, independent of how many trail configurations have this shadow). Further field-theoretical expositions may be found in [23].

2.3. Exact enumeration

The model (trails or silhouettes) consists of l bonds of fixed length, thus connecting $l+1$ monomeric units (with overlaps at intersections) on a face-centred cubic lattice which has a coordination number $q = 12$. The lattice is described by a simple cubic

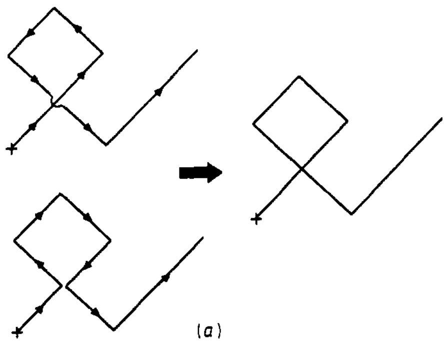

(a)

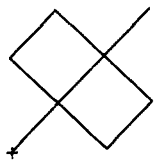

(b)

Figure 2. (*a*) The two trails that have the same silhouette; (*b*) a topologically non-trivial silhouette that has many trails.

lattice with primitive vectors [32]

$$\hat{a}_1 = \frac{1}{\sqrt{2}}(\hat{x}+\hat{y}) \qquad \hat{a}_2 = \frac{1}{\sqrt{2}}(\hat{y}+\hat{z}) \qquad \hat{a}_3 = \frac{1}{\sqrt{2}}(\hat{x}+\hat{z}) \tag{1}$$

and thus each bond is of length unity in units of $|\hat{a}_1| = |\hat{a}_2| = |\hat{a}_3|$.

The enumeration is performed with the first monomeric site fixed at the origin and the first link fixed in the a_1 direction. By carefully considering symmetry factors, there are only four sets of distinct configurations:

(i) a set of one group of configurations (second link along $\hat{a}_1$);

(ii) a set of two groups with the same type of configurations (second link along $\hat{a}_2 - \hat{a}_3$);

(iii) a set of four groups with the same type of configurations (second link along $\hat{a}_3$) and

(iv) another set of four groups with the same type of configurations (second link along $-\hat{a}_1 + \hat{a}_2$).

To save computer time, we enumerate only these four distinct sets from which the total number of configurations can easily be obtained. We shall study the following three main properties of physical importance:

(*a*) the total number of walks (trails or silhouettes) of length l and I intersections, $c(l, I)$;

(*b*) the distribution function, $U_l(\theta)$, and

(*c*) the mean square end-to-end distance, $\langle r_l^2(\theta)\rangle$, where r is the end-to-end distance.

Thus, we define [7, 8, 22, 24]

$$c(l, I) = \sum_r C(l, I, r) \tag{2a}$$

$$d(l, I) = \sum_r r^2 C(l, I, r). \tag{2b}$$

The partition function and the average square end-to-end distance on a lattice are then defined respectively as

$$U_l(\theta) = \sum_{I \geqslant 0} c(l, I)\, e^{I\theta} \tag{3}$$

$$\langle r_l^2(\theta)\rangle = \frac{\Sigma_{I\geqslant 0} d(l, I)\, e^{I\theta}}{\Sigma_{I\geqslant 0} c(l, I)\, e^{I\theta}}. \tag{4}$$

These expressions reduce in the large-l limit to [33, 34]

$$\lim_{l\to\infty} U_l(\theta) \to \Gamma(\theta) l^{\gamma(\theta)-1} \mu^l(\theta) \tag{5}$$

$$\lim_{l\to\infty} \langle r_l^2(\theta)\rangle \to B(\theta) l^{2\nu(\theta)} \tag{6}$$

where we have included the argument θ to show explicitly any possible temperature dependence of the various physical quantities. Amplitudes $\Gamma(\theta)$ and $B(\theta)$ and the growth parameter $\mu(\theta)$ are non-universal quantities. The critical exponents $\gamma(\theta)$ and $\nu(\theta)$ are universal and are expected to assume only three possible values:

(a) $\nu = \nu_{\mathrm{SAW}}$, $\gamma = \gamma_{\mathrm{SAW}}$ for $\theta < \theta_{\mathrm{t}}$ in swollen phase;

(b) $\nu = \nu_{\mathrm{t}}$, $\gamma = \gamma_{\mathrm{t}}$ at the tricritical point $\theta = \theta_{\mathrm{t}}$;

(c) $\nu = 1/d$, $\gamma = \gamma_{\mathrm{c}}$ in the dense phase $\theta > \theta_{\mathrm{t}}$

where d is the dimension of the lattice.

As mentioned in the introduction, trails and silhouettes interpolate between RW and SAW and are thus expected to have some of the virtues and defects of RW and SAW. Another interesting question to ask, then, is: do trails and silhouettes have the infinite memory that SAW have as a result of the excluded volume constraint? This infinite memory raises the important question that if we fix the initial step (along $\boldsymbol{a}_1$, say) will the walks remember the direction of this first step as the length of walks tends to infinity [35-37]? This is the so-called persistency of trails and silhouettes and will also be addressed below.

3. Results from exact enumeration: trails

Tables 1 and 2 present $c(l, I)$ and $d(l, I)$ respectively for the trails up to $l = 10$ for $I = 0$–5. In any exact enumeration involving thousands of graphs, strong evidence

Table 1. Face-centred cube: trail. The coefficients $\frac{1}{12}c(l, I)$.

l	$I=0$	$I=1$	$I=2$	$I=3$	$I=4$	$I=5$
1	1					
2	11					
3	117	4				
4	1 225	102				
5	12 711	1 748	36			
6	131 143	25 366	1 476			
7	1 347 679	336 800	34 122	680		
8	13 808 087	4 236 032	611 152	31 064	176	
9	141 147 827	51 367 620	9 530 578	828 552	20 136	
10	1440 160 797	606 733 924	136 495 818	16 900 552	888 352	7 848

Table 2. Face-centred cube: trail. The coefficients $\frac{1}{12}d(l, I)$.

l	$I=0$	$I=1$	$I=2$	$I=3$	$I=4$	$I=5$
1	1					
2	24					
3	409	0				
4	6 012	80				
5	81 315	3 064	36			
6	1 042 564	72 792	2 016			
7	12 878 367	1 382 636	68 146	512		
8	154 777 460	23 024 640	1 718 152	42 192	176	
9	1 821 449 227	351 548 796	35 895 586	1 651 584	25 976	
10	21 081 182 692	5 047 104 544	660 135 128	45 982 256	1 492 368	8 464

must be adduced that no configurations have been duplicated or omitted. In order to do so, we have checked our numbers corresponding to $I=0$ columns against independent existing literature for SAW [7, 34]. We also note that intersection occurs only for lengths of more than three, as can easily be verified. For $l=3$, the $d(l, I)$ value with $I=1$ is exactly zero because in this case we have only rings and the end-to-end distance is exactly zero. To further check that we have the symmetry factors properly accounted for (see § 2.3) we have enumerated by brute force up to a chain length of 9 and checked against the figures obtained by taking the symmetry factors into account. Exact agreement is obtained in each case.

Analysis of the data proceeds in three stages:

(i) specific heat calculations to locate the tricritical point;

(ii) Dlog Padé extrapolation to extract the critical exponents in large l limit;

(iii) persistency study to see the effect of fixing the initial step.

3.1. *Specific heat*

The 'specific heat' per unit link is defined as†

$$\begin{aligned} h_l(\theta) &= \frac{1}{l}\frac{\partial^2}{\partial\theta^2}\log U_l(\theta) \\ &= \langle I^2(\theta)\rangle - \langle I(\theta)\rangle^2. \end{aligned} \tag{7}$$

This is a measure of relative fluctuations in the number of intersections. It was suggested in [8] (on the Θ point) that the form of the specific heat graphs may be a revealing indicator of the thermodynamical behaviour of a system as the path length $l\to\infty$. Figure 3 shows the specific heat graphs for various path lengths. It is obvious from the plots that, as the path length increases, the specific heat becomes more sharply peaked. This observation is supported by earlier studies in the 2D Ising model [38] and Monte Carlo studies [39]. In the former, it is seen that a similar trend in the specific heat leads to a divergence in the infinite limit, while in the latter the trend

†Note that the usual definition of specific heat per unit link is just $k_B\theta^2 h_l(\theta)$. We shall follow [8] and hereafter refer to $h_l(\theta)$ as the specific heat per unit link. This also explains the non-vanishing 'specific heats' at $\theta=0$.

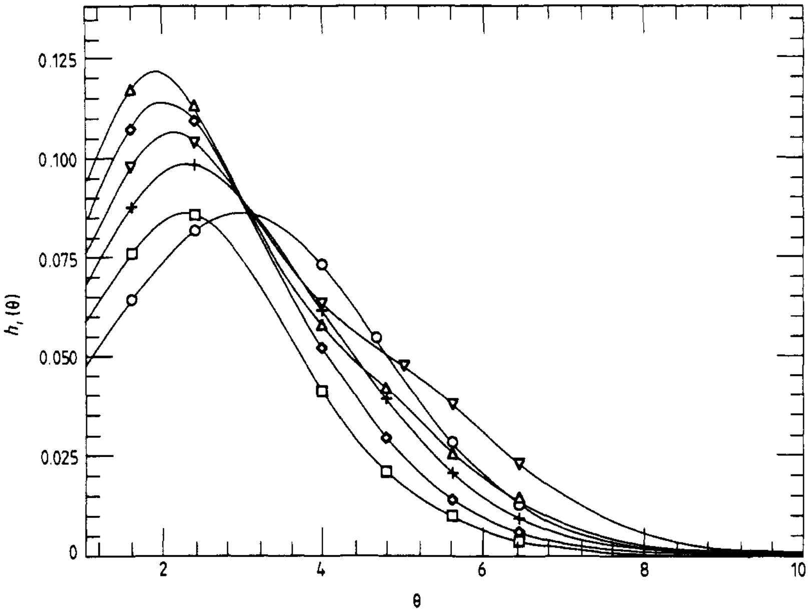

Figure 3. Specific heat plots of the trail problem for $l = 5$–10: ○ $l=5$; □ $l=6$; + $l=7$; ▽ $l=8$; ◇ $l=9$; △ $l=10$.

established by short chains is seen to persist to long path lengths. Since no singular point is expected, the value of θ at which $h_l(\theta)$ diverges is a signature of the tricritical point (confirmation of this claim is the approximate renormalisation group calculations of Burch and Moore [40]). The values of θ corresponding to the maxima of $h_l(\theta)$, $\theta_{\max}$, do not fall on the same point but rather show a regular shift towards lower θ as a function of l. Figure 4 is a plot of the values of θ corresponding to the specific heat maxima against the inverse path length. We linearly extrapolated this to $1/l=0$ or $l \to \infty$ to locate the tricritical point [22, 24]. The linearly extrapolated value is

$$\theta_t = 1.20 \pm 0.05.$$

3.2. Dlog Padé analysis [41, 42]

The Padé approximant method is particularly useful in representing integral functions whose only singularities are poles (i.e. meromorphic functions). A careful study of the functional forms of the large-l limit of the expressions for $U_l(\theta)$ and $\langle r_l^2(\theta)\rangle$ reveals that, in the process of computing the critical exponents, the quantity of interest (for example, equations (5) and (6)) is best calculated via the logarithmic derivatives

$$\begin{aligned} g(x) &= \frac{\mathrm{d}}{\mathrm{d}x}\ln f(x) \\ &= \frac{\mathrm{d}f/\mathrm{d}x}{f(x)} \\ &= \sum_{k=0} d_k x^k \\ &\approx \frac{\gamma}{x_c - x} \end{aligned} \tag{8}$$

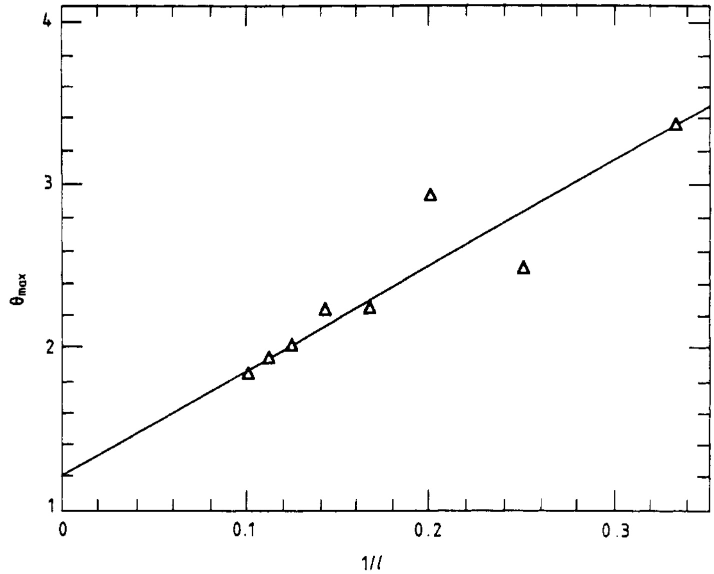

Figure 4. Plot of specific heat maxima, $\theta_{\max}$ against $1/l$ for the trail problem: $\triangle$ are data points; the line is the linear fit.

as $x \to x_c$, where $g(x)$ is now meromorphic, has simple poles and the critical exponents are just the residues. This is the so-called Dlog Padé approximation method. We apply this to the series in (5). In table 3 values of γ and μ are presented for various temperatures in the vicinity of the predicted tricritical point. The exponent ν is similarly obtained from the $\langle r_l^2(\theta)\rangle$ series (6) and is tabulated in table 4. The results, at the best estimate of the tricritical temperature of $\theta_t = 1.20$, are

$$\mu_t = 13.7 \pm 0.1$$

$$\gamma_t = 0.38 \pm 0.03$$

$$\nu_t = 0.51 \pm 0.04$$

Table 3. The exponent γ (and the growth parameter μ) in the vicinity of θ_t of the face-centred cubic lattice. × are defective poles.

$[L/M]$	$I = 1.0$	$I = 1.1$	$I = 1.2$	$I = 1.3$	$I = 1.4$	$I = 1.5$
[3/3]	0.798	0.753	0.704	0.646	0.582	0.509
	(12.354)	(12.640)	(12.966)	(13.345)	(13.788)	(14.311)
[3/4]	0.718	0.671	0.626	0.583	0.544	0.509
	(12.522)	(12.827)	(13.159)	(13.518)	(13.903)	(14.312)
[4/3]	0.749	0.700	0.650	0.600	0.551	0.509
	(12.466)	(12.770)	(13.107)	(13.478)	(13.884)	(14.313)
[4/4]	0.357	×	0.752	0.686	0.593	0.509
	(13.101)	(×)	(12.551)	(13.173)	(13.745)	(14.311)
[4/5]	0.461	0.408	0.360	0.318	0.282	×
	(12.926)	(13.315)	(13.739)	(14.200)	(14.698)	(×)
[5/4]	0.465	0.428	0.407	0.403	0.407	0.413
	(12.920)	(13.279)	(13.637)	(13.985)	(14.317)	(14.651)

Table 4. The exponent ν (and the critical coupling $\mu \equiv 1$) in the vicinity of θ_t of the face-centred cubic lattice. $\times$ are defective poles.

$[L/M]$	$I=1.0$	$I=1.1$	$I=1.2$	$I=1.3$	$I=1.3$	$I=1.5$
[3/3]	0.254	0.240	0.232	0.230	0.236	0.254
	(1.038)	(1.037)	(1.034)	(1.028)	(1.020)	(1.009)
[3/4]	0.406	0.396	0.386	0.375	0.364	0.349
	(0.998)	(0.996)	(0.993)	(0.990)	(0.987)	(0.984)
[4/3]	0.499	0.488	0.473	0.450	0.419	0.379
	(0.981)	(0.978)	(0.976)	(0.976)	(0.977)	(0.979)
[4/4]	0.699	0.822	$\times$	$\times$	$\times$	$\times$
	(0.952)	(0.935)	($\times$)	($\times$)	($\times$)	($\times$)
[4/5]	0.485	0.484	0.482	0.478	0.472	0.464
	(0.981)	(0.977)	(0.973)	(0.968)	(0.964)	(0.960)
[5/4]	0.539	0.544	0.549	0.555	0.559	0.562
	(0.973)	(0.968)	(0.962)	(0.957)	(0.951)	(0.946)

in agreement with [22]. It is to be emphasised that heavier weights are given to the highest Padé approximants and the errors are set by these approximants. The results should be compared with those of the Θ point ($\gamma_\Theta = 1$, $\nu_\Theta = \frac{1}{2}$) [8, 10, 20, 21]. We note that γ_t is substantially smaller than unity, reflecting deviations from Gaussian behaviour and indicating that trails at tricriticality belong to a universality class different from that of SAW.

3.3. *Persistency*

To quantify persistency, we shall investigate whether there is any relation governing this behaviour at constant fugacities ($f = e^{I\theta}$) of zero and unity [37]. Since it is believed that in general all critical exponents can be related to two basic ones, say ν and γ, we further ask whether this relation can be expressed in terms of these characteristic critical exponents of the model [6, 36]. Figure 5 shows how the end-to-end distance along the direction of $\boldsymbol{a}_1$ for a given configuration is measured. The m moment of the

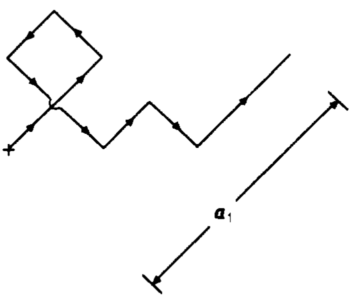

Figure 5. A trail with the initial step fixed along $\boldsymbol{a}_1$. The displacement along $\boldsymbol{a}_1$ is measured to calculate the persistency.

Table 5. Face-centred cube: trail. (a) $\boldsymbol{a}_1(l, I)$ and $\langle\langle \boldsymbol{a}_1\rangle\rangle$; ($b$) $\boldsymbol{a}_1^3(l, I)$ and $\langle\langle \boldsymbol{a}_1^3\rangle\rangle$; ($c$) $\boldsymbol{a}_1^5(l, I)$ and $\langle\langle \boldsymbol{a}_1^5\rangle\rangle$; ($d$) $\boldsymbol{a}_1^7(l, I)$ and $\langle\langle \boldsymbol{a}_1^7\rangle\rangle$.

(a)	$\boldsymbol{a}_1(l, I)$					$\langle \boldsymbol{a}_1(l, I)\rangle$	
l	$I=0$	$I=1$	$I=2$	$I=3$	$I=4$	$f=0$	$f=1$
1	0.100 00E1					0.100 00E1	0.100 00E1
2	0.120 00E2					0.109 09E1	0.109 09E1
3	0.133 00E3	0.000 00E0				0.113 68E1	0.109 92E1
4	0.142 60E4	0.340 00E2				0.116 41E1	0.110 02E1
5	0.150 23E5	0.942 00E3	0.240 00E2			0.118 19E1	0.110 31E1
6	0.156 62E6	0.170 72E5	0.884 00E3			0.119 43E1	0.110 50E1
7	0.162 18E7	0.258 06E6	0.218 62E5	0.212 00E3		0.120 34E1	0.110 62E1
8	0.167 14E8	0.353 35E7	0.426 59E6	0.157 12E5	0.112 00E3	0.121 05E1	0.110 72E1
9	0.171 65E9	0.455 01E8	0.715 05E7	0.498 56E6	0.112 24E5	0.121 61E1	0.110 80E1

(b)	$\boldsymbol{a}_1^3(l, I)$					$\langle \boldsymbol{a}_1^3(l, I)\rangle$	
l	$I=0$	$I=1$	$I=2$	$I=3$	$I=4$	$f=0$	$f=1$
1	0.100 00E1					0.100 00E1	0.100 00E1
2	0.240 00E2					0.218 18E1	0.218 18E1
3	0.421 00E3	0.000 00E0				0.359 83E1	0.347 93E1
4	0.634 45E4	0.355 00E2				0.517 92E1	0.480 78E1
5	0.875 46E5	0.177 00E4	0.150 00E2			0.688 74E1	0.616 29E1
6	0.114 06E7	0.489 68E5	0.146 00E4			0.869 74E1	0.753 89E1
7	0.142 75E8	0.102 87E7	0.532 57E5	0.149 00E3		0.105 92E2	0.893 22E1
8	0.173 44E9	0.184 13E8	0.137 62E7	0.220 90E5	0.640 00E2	0.125 61E2	0.103 42E2
9	0.205 97E10	0.2968 84E9	0.293 24E8	0.108 15E7	0.141 88E5	0.145 93E2	0.117 65E2

(c)	$\boldsymbol{a}_1^5(l, I)$					$\langle \boldsymbol{a}_1^5(l, I)\rangle$	
l	$I=0$	$I=1$	$I=2$	$I=3$	$I=4$	$f=0$	$f=1$
1	0.100 00E1					0.100 00E1	0.100 00E1
2	0.645 00E2					0.586 36E1	0.586 36E1
3	0.187 30E4	0.000 00E0				0.160 09E2	0.154 79E2
4	0.402 29E5	0.358 75E2				0.328 40E2	0.303 43E2
5	0.731 22E6	0.451 20E4	0.127 50E2			0.575 27E2	0.507 59E2
6	0.119 42E8	0.204 20E6	0.349 40E4			0.910 61E2	0.769 04E2
7	0.181 02E9	0.608 30E7	0.200 40E6	0.133 25E3		0.134 32E3	0.108 94E3
8	0.259 70E10	0.143 16E9	0.707 77E7	0.484 94E5	0.520 00E2	0.188 08E3	0.147 02E3
9	0.357 19E11	0.289 28E10	0.193 41E9	0.366 62E7	0.275 89E5	0.253 06E3	0.191 28E3

(d)	$\boldsymbol{a}_1^7(l, I)$					$\langle \boldsymbol{a}_1^7(l, I)\rangle$	
l	$I=0$	$I=1$	$I=2$	$I=3$	$I=4$	$f=0$	$f=1$
1	0.100 00E1					0.100 00E1	0.100 00E1
2	0.198 37E3					0.180 34E2	0.180 34E2
3	0.100 66E5	0.000 00E0				0.860 34E2	0.831 90E2
4	0.314 72E6	0.359 69E2				0.256 91E3	0.237 19E3
5	0.761 41E7	0.135 79E5	0.121 87E2			0.599 02E3	0.526 23E3
6	0.156 82E9	0.105 56E7	0.101 45E5			0.119 58E4	0.999 37E3
7	0.289 02E10	0.454 47E8	0.979 45E6	0.129 31E3		0.214 46E4	0.170 81E4
8	0.490 99E11	0.141 87E10	0.485 90E8	0.136 12E6	0.490 00E2	0.355 58E4	0.270 60E4
9	0.783 71E12	0.360 93E11	0.171 85E10	0.163 04E8	0.682 44E5	0.555 24E4	0.404 91E4

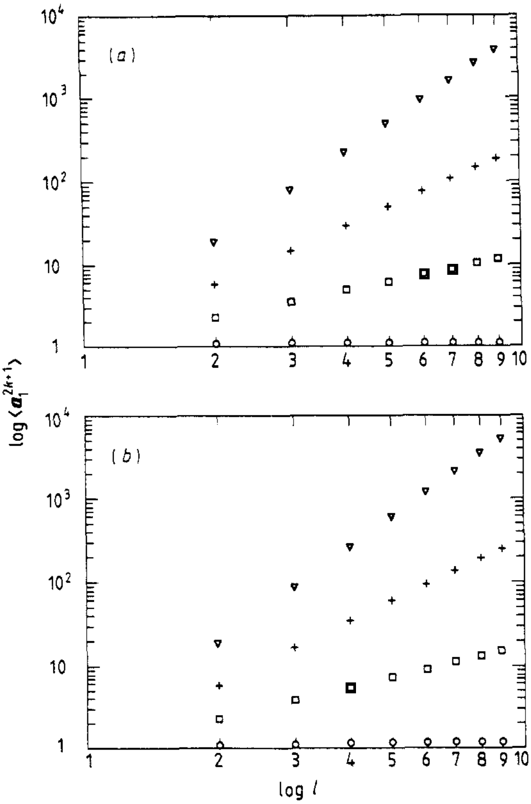

Figure 6. (a) Plots of the odd moments of the persistency along $\boldsymbol{a}_1$ for the trail problem with $f=1$: ○ $k=0$; □ $k=1$; + $k=2$; ▽ $k=3$. (b) The corresponding plots with $f=0$.

persistency in the $\boldsymbol{a}_1$ direction is then defined through the analogue of (2b):

$$\boldsymbol{a}_1^m(l, I)=\sum_r \boldsymbol{a}_1^m C(l, I, r). \tag{9a}$$

The average odd moments of the persistency induced by fixing the direction of the first step is thus defined as

$$\langle \boldsymbol{a}_1^{2k+1}\rangle=\frac{\sum_I \boldsymbol{a}_1^{2k+1}\,\mathrm{e}^{I\theta}}{\sum_I c(l, I)\,\mathrm{e}^{I\theta}}. \tag{9b}$$

In table 5 we tabulate the first four odd moments for trails. As is very obvious in figure 6(a) (fugacity $f=1$) and figure 6(b) (fugacity $f=0$), these moments seem to obey power laws of the form [43, 44]

$$\begin{aligned}&\langle \boldsymbol{a}_1(l)\rangle \sim C\\ &\langle \boldsymbol{a}_1^{2k+1}(l)\rangle \sim l^{mk\nu} \qquad k\geqslant 1\end{aligned} \tag{10}$$

where C is a constant, $\nu=\frac{3}{5}$, $m\simeq 2.0$ in the Malakis-type trails of figure 6(a) and $\nu=\nu_{\mathrm{SAW}}=\frac{3}{5}$, $m\simeq 2.0$ in the SAW-type trails of figure 6(b). It is interesting to note that the results of the Malakis-type trails support the belief that the latter belong to the universality class of SAW. A similar dependence in two dimensions (with the exception of a log factor which is special to two dimensions) has been observed in [37] where the enumeration is performed on a square lattice and a scaling argument is given in its support. It is also to be noted that the reduced moments $\bar{M}^{2k+1} = (\langle a_1^{2k+1}\rangle / \langle a_1\rangle^{2k+1}) \geqslant 1$ where the equality sign holds for a path length of one and the inequality gets larger as the path length increases. It is also seen that the reduced moments increase with the fugacity factor, in accord with the observation of [8].

4. Results from exact enumeration: silhouettes

Tables 6 and 7 present $c(l, I)$ and $d(l, I)$ respectively for the silhouettes up to $l = 10$ for $I = 0$–5. It is observed that the first column of the table ($I = 0$) is exactly that of the corresponding column in the trail table and the second ($I = 1$) is half that of the corresponding column in the trail table. This is as it should be from the definition (see figures 1 and 2). There seems to be no simple relationship relating the number of trails corresponding to a silhouette configuration for $I \geqslant 2$.

Table 6. Face-centred cube: silhouette. The coefficients $\frac{1}{12}c(l, I)$.

l	$I=0$	$I=1$	$I=2$	$I=3$	$I=4$	$I=5$
1	1					
2	11					
3	117	2				
4	1 225	51				
5	12 711	874	6			
6	131 143	12 683	263			
7	1 347 679	168 400	6 377	42		
8	13 808 087	2 118 016	118 170	$1\,900\frac{1}{2}$	4	
9	141 147 827	25 683 810	$1\,890\,138\frac{1}{3}$	52 854	413	
10	1 440 160 797	303 366 962	27 610 184	1 134 352	18 236	$50\frac{1}{12}$

Table 7. Face-centred cube: silhouette. The coefficients $\frac{1}{12}d(l, I)$.

l	$I=0$	$I=1$	$I=2$	$I=3$	$I=4$	$I=5$
1	1					
2	24					
3	409	0				
4	6 012	40				
5	81 315	1 532	6			
6	1 042 564	36 396	336			
7	12 878 367	691 318	11 821	32		
8	154 777 460	11 512 320	310 584	2 596	4	
9	1 821 449 227	175 774 398	6 717 797	102 922	553	
10	21 081 182 692	2 523 552 272	127 086 884	2 955 136	30 932	$56\frac{1}{12}$

4.1. Specific heat

The specific heat plots are depicted in figure 7. Again we observe a regular shift of the peaks as the path length increases. Figure 8 is a plot of θ_{max} against inverse path length. We employ a similar extrapolation described above to locate the tricritical point at $l \to \infty$. The linearly extrapolated value is

$$\theta_t = 2.30 \pm 0.05.$$

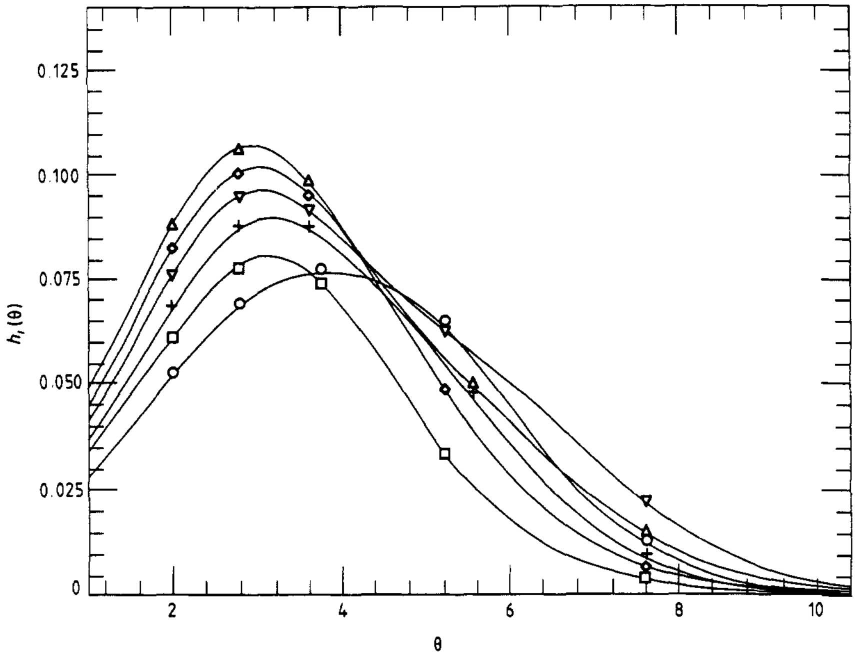

Figure 7. Specific heat plots of the silhouette problem for $l = 5$–10: ○ $l = 5$; □ $l = 6$; + $l = 7$; ▽ $l = 8$; ◇ $l = 9$; △ $l = 10$.

4.2. *Dlog Padé analysis*

The results from the Dlog Padé analysis for μ, γ and ν are presented in tables 8 and 9 respectively. The results, at the best estimate of the tricritical temperature of $\theta_t = 2.30$, are

$$\mu_t = 13.8 \pm 0.2$$
$$\gamma_t = 0.61 \pm 0.03$$
$$\nu_t = 0.45 \pm 0.03$$

consistent with the results of [29, 45]. We emphasise again that heavier weights have been given to the highest Padé approximants and the errors are bounded by these approximants. A few remarks about these tricritical exponents are in order:

(i) the exponents γ_t and ν_t are different from those of trails so we conclude that trails and silhouettes do not belong to the same universality class;

(ii) these exponents are also different from the usual Θ point exponents of $\gamma_\Theta = 1$, $\nu_\Theta = \frac{1}{2}$,

(iii) these results are in reasonable agreement with the predictions of the $\sqrt{\epsilon}$ expansion in $\epsilon = d - 4$ dimensions ($\gamma_\epsilon = 0.8$, $\nu_\epsilon = 0.43$) [23, 29].

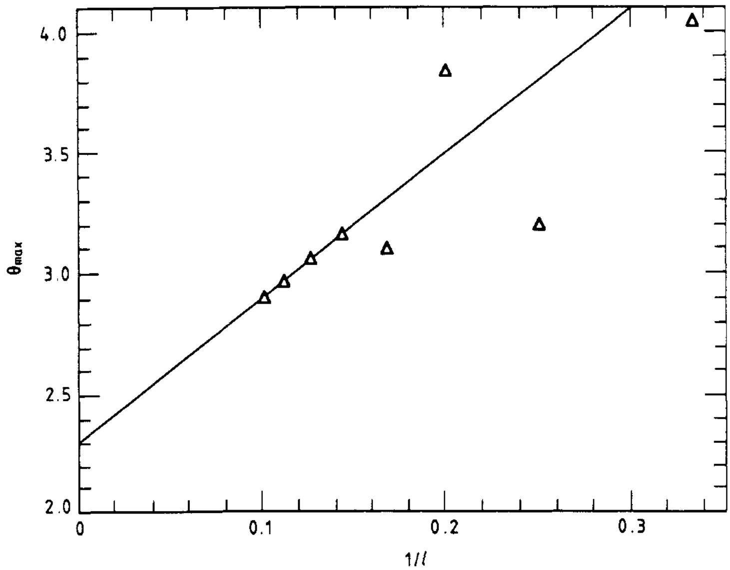

Figure 8. Plot of specific heat maxima, θ_{max}, against $1/l$ for the silhouette problem: △ are data points; the line is the linear fit.

Table 8. The exponent γ (and the growth parameter μ) in the vicinity of θ_t of the face-centred cubic lattice. × are defective poles.

[L/M]	$\theta=2.2$	$\theta=2.3$	$\theta=2.4$	$\theta=2.5$	$\theta=2.6$	$\theta=2.7$
[3/3]	0.708	0.661	0.607	0.547	0.477	0.396
	(13.386)	(13.764)	(14.196)	(14.697)	(15.291)	(16.011)
[3/4]	0.739	0.706	0.672	0.640	0.609	0.578
	(13.296)	(13.624)	(13.976)	(14.355)	(14.760)	(15.193)
[4/3]	0.746	0.720	0.702	0.707	0.809	×
	(13.276)	(13.583)	(13.880)	(14.139)	(14.065)	(×)
[4/4]	0.722	0.683	0.643	0.602	0.562	0.522
	(13.343)	(13.692)	(14.072)	(14.486)	(14.936)	(15.424)
[4/5]	0.640	0.586	0.534	0.485	0.458	0.395
	(13.509)	(13.905)	(14.336)	(14.804)	(15.311)	(15.858)
[5/4]	0.688	0.644	0.602	0.561	0.521	0.483
	(13.425)	(13.791)	(14.187)	(14.615)	(15.077)	(15.574)

4.3. *Persistency*

The odd moments of the persistency are tabulated in table 10 and displayed in figure 9 for the Malakis-type silhouette ($f=1$). The corresponding SAW-type silhouette is exactly the same as that of figure 6(b) since trails and silhouettes are the same at $f=0$ (see § 2). It is obvious that the behaviour of the persistency is similar to that of trails, except that $(\langle a_1^{2k+1}\rangle)_{\text{trail}} \leq (\langle a_1^{2k+1}\rangle)_{\text{silhouette}}$. Though the difference is not quite appreciable up to the maximum path length we consider here, it is evident that the 'discrepancy' gets larger as the path length increases. This is expected and may be

Table 9. The exponent ν (and the critical coupling $\mu \equiv 1$) in the vicinity of θ_t of the face-centred cubic lattice. $\times$ are defective poles.

$[L/M]$	$\theta=2.2$	$\theta=2.3$	$\theta=2.4$	$\theta=2.5$	$\theta=2.6$	$\theta=2.7$
[3/3]	0.259	0.272	0.293	0.318	0.348	0.377
	(1.025)	(1.017)	(1.007)	(0.997)	(0.986)	(0.975)
[3/4]	0.272	0.250	0.222	0.184	$\times$	$\times$
	(1.021)	(1.023)	(1.024)	(1.028)	($\times$)	($\times$)
[4/3]	0.272	0.251	0.234	0.225	0.227	0.238
	(1.021)	(1.022)	(1.021)	(1.019)	(1.015)	(1.008)
[4/4]	0.258	0.271	0.284	0.299	0.315	0.331
	(1.025)	(1.017)	(1.001)	(1.002)	(0.995)	(0.987)
[4/5]	0.413	0.404	0.395	0.388	0.381	0.377
	(0.990)	(0.988)	(0.985)	(0.983)	(0.981)	(0.977)
[5/4]	0.499	0.493	0.481	0.464	0.440	0.415
	(0.976)	(0.974)	(0.972)	(0.971)	(0.971)	(0.972)

explained as follows. For a fixed chain length, the chain can be quite 'open' with few intersections or can be quite 'collapse' with many intersections. If we recall that a silhouette with many intersections can have multiple trails, then we see that these 'collapse' (and thus smaller $|\hat{\boldsymbol{a}}_1|$) configurations are more heavily weighted (by the multiplicity) in the trail configurations than in the silhouette configurations. For longer chain lengths, this happens even more often and thus the discrepancy becomes larger. It is rather unfortunate that we can make no quantitative deduction about this ratio from the short chains we have generated here.

5. Conclusions

In the present paper, we have tabulated the face-centred cubic lattice series for the number of configurations and end-to-end distance for trails and silhouettes according to their chain lengths and number of intersections. We have also computed the 'specific heat' (mean-square fluctuations in the number of intersections) and shown the existence of tricritical points as the fugacity for intersection is increased. The maxima in the specific heat exhibit a regular trend towards lower values of θ as the order l in the series increases. We perform a linear regression to extrapolate the value of θ_t and deduce the best bounds on the tricritical exponents for both the trails and silhouettes.

Our results, though extracted from series of short path length ($l=10$), are quite stable due to the fact that the embedding lattice is close-packed (face-centred cubic lattice). The tricritical exponents obtained show that the behaviour of trails at tricriticality is non-Gaussian and that the tricritical point is distinct from the usual Θ point. Despite the supporting evidence in favour of a new tricritical behaviour for trails, this fact does not, *ipso facto*, rule out other possibilities like a fast crossover with rapid variation in various quantities (but no singularities) or a tricritical behaviour analogous to standard tricritical polymers. We hope that the open questions will stimulate a more accurate determination of the tricritical properties for this special point which is inaccessible by renormalisation group and is not described by a perturbative fixed point in $4-\epsilon$ dimensions.

Table 10. Face-centred cube: silhouette. (*a*) $\boldsymbol{a}_1(l, I)$ and $\langle(\boldsymbol{a}_1)\rangle$; (*b*) $\boldsymbol{a}_1^3(l, I)$ and $\langle(\boldsymbol{a}_1^3)\rangle$; (*c*) $\boldsymbol{a}_1^5(l, I)$ and $\langle(\boldsymbol{a}_1^5)\rangle$; (*d*) $\boldsymbol{a}_1^7(l, I)$ and $\langle(\boldsymbol{a}_1^7)\rangle$.

(*a*)	$\boldsymbol{a}_1(l, I)$					$\langle \boldsymbol{a}_1(l, I)\rangle$	
l	$I=0$	$I=1$	$I=2$	$I=3$	$I=4$	$f=0$	$f=1$
1	0.100 00E1					0.100 00E1	0.100 00E1
2	0.120 00E2					0.109 09E1	0.109 09E1
3	0.133 00E3	0.000 00E0				0.113 68E1	0.111 76E1
4	0.142 60E4	0.170 00E2				0.116 41E1	0.113 09E1
5	0.150 23E5	0.471 00E3	0.400 00E1			0.118 19E1	0.114 03E1
6	0.156 62E6	0.853 60E4	0.147 33E3			0.119 43E1	0.114 72E1
7	0.162 18E7	0.129 03E6	0.376 13E4	0.132 50E2		0.120 34E1	0.115 25E1
8	0.167 14E8	0.176 67E7	0.763 43E5	0.976 92E3	0.254 55E1	0.121 05E1	0.115 65E1
9	0.171 65E9	0.227 51E8	0.132 51E7	0.311 48E5	0.236 02E3	0.121 61E1	0.115 99E1

(*b*)	$\boldsymbol{a}_1^3(l, I)$					$\langle \boldsymbol{a}_1^3(l, I)\rangle$	
l	$I=0$	$I=1$	$I=2$	$I=3$	$I=4$	$f=0$	$f=1$
1	0.100 00E1					0.100 00E1	0.100 00E1
2	0.240 00E2					0.218 18E1	0.218 18E1
3	0.421 00E3	0.000 00E0				0.359 83E1	0.353 78E1
4	0.634 45E4	0.177 50E2				0.517 92E1	0.498 61E1
5	0.875 46E5	0.885 00E3	0.250 00E1			0.688 74E1	0.650 68E1
6	0.114 06E7	0.244 84E5	0.243 33E3			0.869 74E1	0.808 76E1
7	0.142 75E8	0.514 37E6	0.900 98E4	0.931 25E1		0.105 92E2	0.971 98E1
8	0.173 44E9	0.920 64E7	0.239 03E6	0.137 66E4	0.145 45E1	0.125 61E2	0.113 98E2
9	0.205 97E10	0.148 42E9	0.524 66E7	0.673 06E5	0.310 75E3	0.145 93E2	0.131 15E2

(*c*)	$\boldsymbol{a}_1^5(l, I)$					$\langle \boldsymbol{a}_1^5(l, I)\rangle$	
l	$I=0$	$I=1$	$I=2$	$I=3$	$I=4$	$f=0$	$f=1$
1	0.100 00E1					0.100 00E1	0.100 00E1
2	0.645 00E2					0.586 36E1	0.586 36E1
3	0.187 30E4	0.000 00E0				0.160 09E2	0.157 39E2
4	0.402 29E5	0.179 37E2				0.328 40E2	0.315 41E2
5	0.731 22E6	0.225 60E4	0.212 50E1			0.575 27E2	0.539 68E2
6	0.119 42E8	0.102 10E6	0.582 33E3			0.910 61E2	0.835 92E2
7	0.181 02E9	0.304 15E7	0.335 37E5	0.832 81E1		0.134 32E3	0.120 92E3
8	0.259 70E10	0.715 81E8	0.120 35E7	0.302 72E4	0.181 81E1	0.188 08E3	0.166 38E3
9	0.357 19E11	0.144 64E10	0.336 61E8	0.228 12E6	0.617 15E3	0.253 06E3	0.220 41E3

(*d*)	$\boldsymbol{a}_1^7(l, I)$					$\langle \boldsymbol{a}_1^7(l, I)\rangle$	
l	$I=0$	$I=1$	$I=2$	$I=3$	$I=4$	$f=0$	$f=1$
1	0.100 00E1					0.100 00E1	0.100 00E1
2	0.198 37E3					0.180 34E2	0.180 35E2
3	0.100 66E5	0.000 00E0				0.860 34E2	0.845 88E2
4	0.314 72E6	0.179 84E2				0.256 91E3	0.246 66E3
5	0.761 41E7	0.678 94E4	0.203 12E1			0.599 02E3	0.560 73E3
6	0.156 82E9	0.527 78E6	0.169 08E4			0.119 58E4	0.109 20E4
7	0.289 02E10	0.227 24E8	0.163 38E6	0.808 20E1		0.214 46E4	0.191 34E4
8	0.490 99E11	0.709 36E9	0.816 92E7	0.850 37E4	0.111 36E1	0.355 58E4	0.310 46E4
9	0.783 71E12	0.180 47E11	0.293 57E9	0.101 57E7	0.154 16E4	0.555 24E4	0.475 22E4

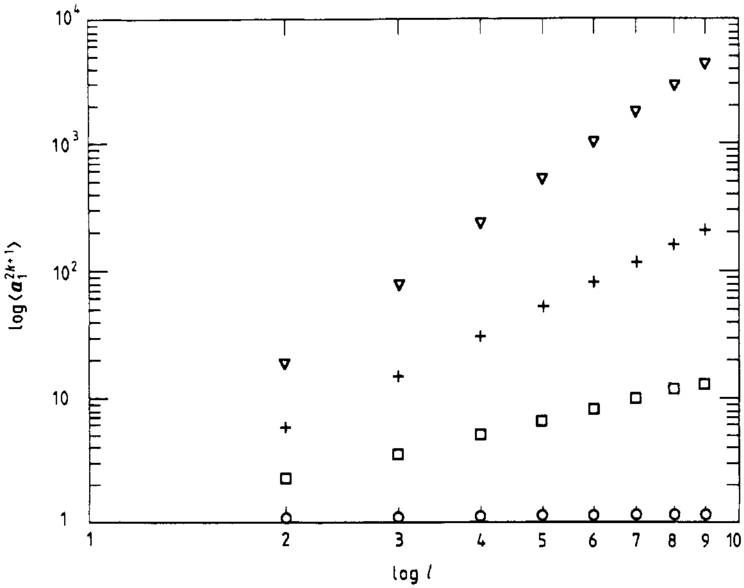

Figure 9. Plots of the odd moments of the persistency along a_1 for the silhouette problem with $f=1$: ○ $k=0$; □ $k=1$; + $k=2$; ▽ $k=3$.

The silhouette results, however, support the renormalisation group $\sqrt{\epsilon}$ expansion predictions extrapolated to $\epsilon=1$. Of particular interest are the confirmation of the non-Gaussian behaviour at the tricritical point ($\nu_t<\frac{1}{2}$ and $\gamma_t<1$) and the confirmation that this tricritical point is distinct from the usual Θ point [7, 8, 19-21].

The tricritical exponents of trails and silhouettes also show that they do not share the same tricritical exponents, indicating that they belong to different universality classes. However, longer series or alternative methods like Monte Carlo or finite-size scaling will be necessary to extract more precise exponents to further confirm these claims [46].

The interesting property of persistency arising from fixing the initial step in a certain fixed direction is also studied. The results show that the persistency may be quantified as a power law in terms of the path length, l, and the critical exponent, ν. As a by-product, we have also indirectly shown that trails and silhouettes at $T=\infty$ (Malakis type) belong to the SAW universality class.

Acknowledgments

The author is very grateful to Dr A Guha (AT&T) and Dr Y Shapir (Rochester) who introduced him to the subject, Dr H Meirovitch (Weizmann) for fruitful discussions and Professor D Duke (SCRI) who has saved the author a factor of six in computer runtime. Assistance from the Supercomputer Computations Research Institute staff, Dr S Youssef and Mr J Sollohub is also fully acknowledged. The author also thanks Miss D E Middleton for her excellent typing.

This work is partially supported by the US Department of Energy under contract no DE-FC05-85ER250000.

References

[1] Malakis A 1976 *J. Phys. A: Math. Gen.* **9** 1283
[2] Massih A R and Moore M A 1975 *J. Phys. A: Math. Gen.* **8** 237
[3] Guttmann A J 1985 *J. Phys. A: Math. Gen.* **18** 567
[4] Grassberger P 1982 *Z. Phys.* B **48** 255
[5] Flory P J 1949 *J. Chem. Phys.* **17** 303
[6] de Gennes, P G 1979 *Scaling Concepts in Polymer Physics* (Ithaca, NY: Cornell University Press)
[7] Rapaport D C 1976 *J. Phys. A: Math. Gen.* **9** 1521
[8] Rapaport D C 1977 *J. Phys. A: Math. Gen.* **10** 637
[9] McCrackin P, Mazur J and Guttmann C L 1973 *Macromol.* **6** 859
[10] Kremer K, Baumgärtner A and Binder K 1982 *J. Phys. A: Math. Gen.* **15** 2879
[11] Baumgärtner A 1982 *J. Physique* **43** 1407
[12] Ishinabe T 1985 *J. Phys. A: Math. Gen.* **18** 3181
[13] Privman V 1986 *Macromol.* **19** 2377
[14] Privman V 1986 *J. Phys. A: Math. Gen.* **19** 3287
[15] Derrida B and Saleur H 1985 *J. Phys. A: Math. Gen.* **18** 1075
[16] Duplantier B and Saleur H 1987 *Phys. Rev. Lett.* **59** 539
[17] Saleur H 1987 *Phys. Rev.* B **35** 3657
[18] Oono Y and Oyama T 1978 *J. Phys. Soc. Japan* **49** 301
[19] Riedel E K and Wegner F J 1972 *Phys. Rev. Lett.* **29** 349
[20] Stephen M J and McCauley J L Jr 1973 *Phys. Lett.* **44A** 89
[21] Stephen M J 1975 *Phys. Lett.* **53A** 363
[22] Guha A, Lim H A and Shapir Y 1988 *J. Phys. A: Math. Gen.* **21** 1043
[23] Shapir Y and Oono Y 1984 *J. Phys. A: Math. Gen.* **17** L39
[24] Lim H A, Guha A and Shapir Y 1988 *J. Phys. A: Math. Gen.* **21** 773
[25] Lim H A, Guha A and Shapir Y 1988 *Phys. Rev.* A in press
[26] Cates M E and Witten T A 1986 *Macromol.* **19** 732
[27] Lundberg R D 1978 *Polym. Prep. Am. Chem. Soc. Div. Polym. Chem.* **19** 455
[28] Moore M A 1977 *J. Phys. A: Math. Gen.* **10** 305
[29] Shapir Y, Guha A and Lim H A 1988 *Phys. Rev. Lett.* submitted
[30] de Gennes P G 1972 *Phys. Lett.* **38A** 339
[31] Domb C 1960 *Adv. Phys.* **9** 149
[32] Ashcroft N W and Mermin N D 1975 *Solid State Physics* (London: Holt-Saunders)
[33] McKenzie D S 1975 *Phys. Rep.* **27C** 37
[34] Domb C 1969 *Stochastic Processes in Chemical Physics* ed K E Shuler (New York: Interscience) p 229
[35] Yamakawa H 1971 *Modern Theory of Polymer Solution* (New York: Harper and Row)
[36] Grassberger P 1982 *Phys. Lett.* **89A** 381
[37] Redner S and Privman V 1987 *J. Phys. A: Math. Gen.* **20** L857
[38] Ferdinand A E and Fisher M E 1969 *Phys. Rev.* **185** 832
[39] Mazur J and McCrackin F L 1968 *J. Chem. Phys.* **49** 648
[40] Burch D J and Moore M A 1976 *J. Phys. A: Math. Gen.* **9** 435
[41] Baker J A 1965 *Advances in Theoretical Physics* ed K A Brueckner (New York: Academic) p 1
[42] Fisher M E 1976 *Statistical Mechanics and Statistical Methods in Theory and Application* ed U Landman (New York: Plenum) p 3
[43] Privman V 1988 private communication
[44] Redner S 1988 private communication and forthcoming paper
[45] Shapir Y, Ramaswamy S, Lim H A and Guha A 1987 unpublished
[46] Meirovitch H and Lim H A 1988 *Phys. Rev.* A **38** 1670